Inorg. Chem. **2002**, *41*, 5882–5890

Bond Dissociation Energies and Structures of $CuNO^+$ and $Cu(NO)_2^+$

Konrad Koszinowski,[†] Detlef Schröder,[†] Helmut Schwarz,[†] Max C. Holthausen,*[,‡] Joachim Sauer,[§] Hideya Koizumi,[||] and P. B. Armentrout*[,||]

Institut für Chemie, Technische Universität Berlin, Strasse des 17. Juni 135, 10623 Berlin, Germany, Fachbereich Chemie der Philipps-Universität Marburg, Hans-Meerwein-Strasse, 35032 Marburg, Germany, Institut für Chemie der Humboldt-Universität zu Berlin, Unter den Linden 6, 10099 Berlin, Germany, and Department of Chemistry, University of Utah, Salt Lake City, Utah 84112

Received May 3, 2002

The bond dissociation energies of $CuNO^+$, $Cu(NO)_2^+$, and $CuAr^+$ are determined by means of guided ion beam mass spectrometry and quantum chemical calculations. From the experiment, the values $D_0(Cu^+–NO) = 1.13 \pm 0.05$, $D_0(ONCu^+–NO) = 1.12 \pm 0.06$, $D_0(Cu^+–Ar) = 0.50 \pm 0.07$, and $D_0(Cu^+–Xe) = 1.02 \pm 0.06$ eV are obtained. The computational approaches corroborate these results and provide additional structural data. The relative values of $D_0(Cu^+–NO)$ and $D_0(Cu^+–Xe)$ are consistent with the approximately thermoneutral formation of $CuXe^+$ upon interacting $CuNO^+$ with xenon. The sequential bond dissociation energies of $Cu(NO)_2^+$ exhibit a trend similar to those of other Cu(I) complexes described in the literature. Although metathesis of nitric oxide to N_2 and O_2 is of considerable interest, no evidence for N–N- or O–O-bond formations in $Cu(NO)_n^+$ ions (with n up to 3) is obtained within the energy range studied experimentally.

1. Introduction

Recently, there has been an ongoing interest in the interactions of nitric oxide (NO) and transition-metal ions.[1−4] Bare copper ions have received particular attention because certain copper-exchanged zeolites serve as efficient catalysts for the decomposition of the air-pollutant NO in the deNO_x process, reaction 1.[5,6]

$$2NO \rightarrow N_2 + O_2 \quad \Delta_r H_{298} = -1.89 \text{ eV} \qquad (1)$$

Moreover, copper ions also play a crucial role in controlling NO_x redox chemistry in biological denitrification.[7]

Stimulated by the first experimental evidence for the existence of $CuNO^+$ as well as its neutral counterpart in the gas phase,[8] major computational efforts were taken to characterize the binding mode in $CuNO^+$ as a prototype metal-ion/molecule complex of nitric oxide.[2,9−13] Whereas low-level HF and CISD computations erroneously predicted a linear $^2\Pi$ ground state,[11] all other studies agree on a bent structure for ground-state $CuNO^+$ ($^2A'$) with this isomer being significantly more stable than the $CuON^+$ species in its $^2A'$ ground state. However, the computed binding energies of $CuNO^+$ strongly depend on the choice of the theoretical method, spanning a range from 0.84, 0.94, and 1.04 eV (all CCSD(T))[2,9,10] and 1.34 eV (B3LYP)[10] up to 1.63 eV (BP86).[14]

* To whom correspondence should be addressed. E-mail: armentrout@chem.utah.edu (P.B.A.).
[†] Technische Universität Berlin.
[‡] Philipps-Universität Marburg.
[§] Humboldt-Universität zu Berlin.
[||] University of Utah.

(1) Feldman, P. L.; Griffith, O. W.; Stuehr, D. J. *Chem. Eng. News* **1993**, *71* (51), 26.
(2) Thomas, J. L. C.; Bauschlicher, C. W., Jr.; Hall, M. B. *J. Phys. Chem. A* **1997**, *101*, 8530.
(3) Smirniotis, P. G.; Peña, D. A.; Uphade, B. S. *Angew. Chem.* **2001**, *113*, 2537; *Angew. Chem., Int. Ed.* **2001**, *40*, 2479.
(4) *Chem. Rev.* **2002**, *102*, 857. The April issue deals with the chemistry of nitric oxide.
(5) Iwamoto, M.; Hamada, H. *Catal. Today* **1991**, *10*, 57.
(6) Dědeček, J.; Bortnovsky, O.; Vondrová, A.; Wichterlová, B. *J. Catal.* **2001**, *200*, 160.
(7) Wasser, I. M.; de Vries, S.; Moënne-Loccoz, P.; Schröder, I.; Karlin, K. D. *Chem. Rev.* **2002**, *102*, 1201.
(8) Sülzle, D.; Schwarz, H.; Moock, K. H.; Terlouw, J. K. *Int. J. Mass Spectrom. Ion Process.* **1991**, *108*, 269.
(9) Hrušák, J.; Koch, W.; Schwarz, H. *J. Chem. Phys.* **1994**, *101*, 3898.
(10) Nachtigallová, D.; Davidová, M.; Nachtigall, P. *Collect. Czech. Chem. Commun.* **1998**, *63*, 1202.
(11) Benjelloun, A. T.; Daoudi, A.; Berthier, G.; Rolando, C. *J. Mol. Struct. (THEOCHEM)* **1996**, *360*, 127.
(12) Blanchet, C.; Duarte, H. A.; Salahub, D. R. *J. Chem. Phys.* **1997**, *106*, 8778.
(13) Zhou, M.; Andrews, L. *J. Phys. Chem. A* **2000**, *104*, 2618.

10.1021/ic020315a CCC: $22.00 © 2002 American Chemical Society
Published on Web 10/05/2002

This unsatisfactory situation prompted us to reinvestigate the Cu^+/NO system in a combined mass-spectrometric and quantum-chemical study aimed toward a consistent determination of the thermochemistry of $Cu(NO)_n^+$ for $n = 1$ and 2. Additional information is obtained for the Cu(I) rare-gas complexes $CuAr^+$ and $CuXe^+$, which were observed in the course of the experiments.

2. Experimental and Theoretical Procedures

Guided Ion Beam (GIB). The reactions of interest were studied using a GIB mass spectrometer described elsewhere.[15,16] Briefly, Cu^+ ions produced by Ar^+-sputtering from a copper cathode entered a 1-m-long flow tube filled with a mixture of helium and argon ($p_{total} \approx 50$ Pa) with small amounts of NO (<1%). Although the efficiency of association between Cu^+ and nitric oxide is unfortunately quite poor under these conditions, the desired ions thereby formed and thermalized, $CuNO^+$ and $Cu(NO)_2^+$, could be mass-selected by a magnet and directed into an octopole ion beam guide providing them with well-defined, tuneable kinetic energies. The octopole passes through a gas cell functioning as a reaction chamber that contained the neutral reactants (argon, xenon, and NO) at pressures of ca. 10−30 mPa. Particular care was taken to purify NO from traces of NO_2 by distillation at temperatures below the melting point of N_2O_4. After passing through the octopole, reactant and product ions were mass analyzed by a quadrupole mass filter and detected. The data are converted from raw data to product cross sections as functions of center-of-mass energies $\sigma(E)$, as detailed previously.[15]

To model the kinetic energy dependence of the cross sections, well-documented routines utilizing eq 2 were adopted:[17−19]

$$\sigma(E) = \sigma_0 \Sigma g_i (E + E_i - E_0)^n / E \qquad (2)$$

Here, E is the relative kinetic energy of the reactants, E_0 is the reaction threshold at 0 K, σ_0 is a scaling parameter, and n is a fitting parameter. The summation is over the rovibrational states of the reactants having internal energies E_i and populations g_i ($\Sigma g_i = 1$). Vibrational frequencies and rotational constants of nitric oxide were taken from the literature,[20] whereas those of $CuNO^+$ and $Cu(NO)_2^+$ were adopted from the calculations reported below. After convolution of eq 2 with the kinetic energy distributions of the reactants (Gaussian shape for the ionic species and Maxwell−Boltzmann for the neutrals), least-squares fits were performed that provided optimized values for σ_0, E_0, and n. To account for lifetime effects that may be operative because of the limited experimental time window available for the course of reaction (approximately 10^{-4} s), eq 2 also was modified by incorporating Rice−Ramsperger−Kassel−Marcus (RRKM) theory as detailed elsewhere.[21,22] However, this effect was essentially negligible (see below), and the methodology is therefore not further outlined here.

Quantum-Chemical Calculations. At the density functional theory (DFT) level, the B3LYP functional as implemented in Gaussian 98 has been applied for geometry optimizations and evaluations of harmonic vibrational frequencies[23] in combination with two different basis sets. The first, denoted B1, was derived from the (14s9p5d) primitive set of Wachters supplemented with two scaled diffuse p-functions[24] and one diffuse d-function as recommended by Hay[25] and contracted according to (6,2,1,1,1,1,1|3,3,1,2,1|3,1,1,1) → [8s5p4d]. For $CuNO^+$, $CuAr^+$, $CuXe^+$, and the low-lying $Cu(NO)_2^+$ isomers, a second basis set (B2) using the Stuttgart/Dresden relativistic effective core potentials was applied, substituting 10 core electrons of Cu[26] and 46 core electrons of Xe,[27] respectively. The corresponding basis sets were contracted (3,1,1,1,1,1|2,2,1,1,1|4,1,1) → [6s5p3d] for Cu and (3,1,1,1|3,1,1,1|1,1,1|1) → [4s4p3d1f] for Xe. Both sets were combined with the standard 6-311+G(d) basis sets for N, O, and Ar.

Additional CCSD(T) single-point calculations were performed on B3LYP/B1-optimized geometries. In these calculations, a larger atomic natural orbital (ANO) basis[28] of the form (19,19,19,19,19,-19,1|14,14,14,14,14,1|10,10,10,10|6,6|4) → [7s6p4d2f1g] has been used for copper. In combination with the correlation-consistent cc-pVTZ basis sets of Dunning for N and O,[29] which were contracted according to (10,10,1,1|5,1,1|1,1|1) → [4s3p2d1f], this is referred to as B3. Relativistic effects were evaluated perturbationally (Darwin and mass-velocity terms) on the basis of the HF/B3 wave function. The CCSD(T) calculations (RCCSD(T) based on ROHF wave functions for open-shell species) were performed using the program MOLPRO.[30]

In all cases, geometry optimizations were performed by applying symmetry constraints as indicated in the figures below. All stationary points were characterized as minima by analytical evaluations of the Hessian matrixes, and harmonic frequencies were computed from the Hessians by standard routines implemented in the Gaussian code. Unscaled B3LYP/B2 values were used for zero-point vibrational energy corrections and thermal corrections for ΔH and ΔG (298 K → 0 K) in the analysis of the experimental data.

(14) Yokomichi, Y.; Yamabe, T.; Ohtsuka, H.; Kakumoto, T. *J. Phys. Chem.* **1996**, *100*, 14424.
(15) Ervin, K. M.; Armentrout, P. B. *J. Chem. Phys*. **1985**, *83*, 166.
(16) Schultz, R. H.; Armentrout, P. B. *Int. J. Mass Spectrom. Ion Process.* **1991**, *107*, 29.
(17) Schultz, R. H.; Crellin, K. C.; Armentrout, P. B. *J. Am. Chem. Soc.* **1991**, *113*, 8590.
(18) Armentrout, P. B. In *Advances in Gas-Phase Ion Chemistry*; Adams, N. G., Babock, L. M., Eds.; JAI Press: Greenwich, CT, 1992; Vol. 1, p 83.
(19) Armentrout, P. B. *Int. J. Mass Spectrom*. **2000**, *200*, 219.
(20) Herzberg, G. *Molecular Spectra and Molecular Structure*, 2nd ed.; Krieger Publishing: Malabar, India, 1989; Vol. 1, p 558 (reprint edition).
(21) Khan, F. A.; Clemmer, D. E.; Schultz, R. H.; Armentrout, P. B. *J. Phys. Chem*. **1993**, *97*, 7978.
(22) Rodgers, M. T.; Ervin, K. M.; Armentrout, P. B. *J. Chem. Phys*. **1997**, *106*, 4499.
(23) Frisch, M. J.; Trucks, G. W.; Schlegel, H. B.; Scuseria, G. E.; Robb, M. A.; Cheeseman, J. R.; Zakrzewski, V. G.; Montgomery, J. A., Jr.; Stratmann, R. E.; Burant, J. C.; Dapprich, S.; Millam, J. M.; Daniels, A. D.; Kudin, K. N.; Strain, M. C.; Farkas, O.; Tomasi, J.; Barone, V.; Cossi, M.; Cammi, R.; Mennucci, B.; Pomelli, C.; Adamo, C.; Clifford, S.; Ochterski, J.; Petersson, G. A.; Ayala, P. Y.; Cui, Q.; Morokuma, K.; Malick, D. K.; Rabuck, A. D.; Raghavachari, K.; Foresman, J. B.; Cioslowski, J.; Ortiz, J. V.; Baboul, A. G.; Stefanov, B. B.; Liu, G.; Liashenko, A.; Piskorz, P.; Komaromi, I.; Gomperts, R.; Martin, R. L.; Fox, D. J.; Keith, T.; Al-Laham, M. A.; Peng, C. Y.; Nanayakkara, A.; Gonzalez, C.; Challacombe, M.; Gill, P. M. W.; Johnson, B.; Chen, W.; Wong, M. W.; Andres, J. L.; Gonzalez, C.; Head-Gordon, M.; Replogle, E. S.; Pople, J. A. *Gaussian 98*, revision A.7; Gaussian, Inc.: Pittsburgh, PA, 1998.
(24) Wachters, A. J. H. *J. Chem. Phys*. **1970**, *52*, 1033.
(25) Hay, P. J. *J. Chem. Phys*. **1977**, *66*, 4377.
(26) Dolg, M.; Wedig, U.; Stoll, H.; Preuss, H. *J. Chem. Phys*. **1987**, *86*, 866.
(27) Nicklass, A.; Dolg, M.; Stoll, H.; Preuss, H. *J. Chem. Phys*. **1995**, *102*, 8942.
(28) Bauschlicher, C. W., Jr. *Theor. Chim. Acta* **1995**, *92*, 183.
(29) Dunning, T. H., Jr. *J. Chem. Phys*. **1989**, *90*, 1007.
(30) MOLPRO V. 2000.1. MOLPRO is a package of ab initio programs written by H.-J. Werner and P. J Knowles with contributions from R. D. Amos, A. Berning, D. L. Cooper, M. J. O. Deegan, A. J. Dobbyn, F. Eckert, C. Hampel, G. Hetzer, T. Leininger, R. Lindh, A. W. Lloyd, W. Meyer, M. E. Mura, A. Nicklass, P. Palmieri, K. Peterson, R. Pitzer, P. Pulay, G. Rauhut, M. Schütz, H. Stoll, A. J. Stone, T. Thorsteinsson.

3. Results

3.1. $CuNO^+$ Cation: Experiment. As expected, the reaction of $CuNO^+$ with the rare gases (Rg) argon and xenon under GIB conditions leads to collision-induced dissociation (CID) according to reaction 3 as well as ligand exchange according to reaction 4.

$$CuNO^+ + Rg \rightarrow Cu^+ + NO + Rg \quad (3)$$

$$CuNO^+ + Rg \rightarrow CuRg^+ + NO \quad (4)$$

Qualitative consideration of the experimental data (Figure 1) shows similar cross sections of reaction 3 for argon and xenon. Slightly more efficient CID with the latter is readily explained by the different polarizabilities of the neutrals,[31,32] $\alpha(Ar) = 1.63 \times 10^{-30}$ m^3 and $\alpha(Xe) = 4.01 \times 10^{-30}$ m^3.[33] The apparent thresholds of reaction 3 coincide for both argon and xenon, consistent with the view that the neutrals only act as collision partners in CID. In marked contrast, the cross sections associated with ligand exchange in reaction 4 differ significantly. In the case of argon, the reaction exhibits a threshold after which the efficiency rises with increasing energy, whereas the cross section declines right from the lowest energies in the experiment with xenon. The $CuXe^+$ cross section follows the energy dependence predicted by the Langevin−Gioumousis−Stevenson model for collisions of ions with polarizable neutrals,[34] except its magnitude is 10% of this prediction. The latter finding indicates an endothermic ligand exchange, whereas the former is typical of an exothermic or near-thermoneutral reaction. This difference in thermochemical quantities probed in both experiments also affects the effective temperatures of the products formed. At the threshold of an endothermic process, the reaction consumes the whole energy available to the reactants, thus providing products having rovibrational temperatures of 0 K. Hence, entropic features do not play a role. On the contrary, no energy needs to be consumed to drive an exothermic reaction at the lowest energies, such that the products can be formed at or even above room temperature and may accordingly be rovibrationally excited. A precise knowledge of the temperature of the products is not necessary, however, because the cross section for ligand exchange with xenon is not quantitatively analyzed here using eq 2. Whereas entropic effects are often negligible for ligand-exchange reactions, the situation changes upon the participation of atomic species.[35] When the rare-gas atom forms a complex with Cu^+ while an NO molecule is released, one vibrational degree of freedom is transformed into a rotation. Because of the smaller energy spacing between rotational levels compared to vibrations, a significant increase of the system's sum of states occurs at room temperature, causing a nonnegligible entropic contribution at thermal energies.

In the reaction of $CuNO^+$ with NO (Figure 1c), only CID in analogy to reaction 3 is observed. Ligand exchange forms products that are degenerate with the reactants and cannot be monitored without isotopic labeling of nitric oxide. Consistent with $\alpha(NO) = 1.74 \times 10^{-30}$ m^3,[33] the CID efficiency for NO is slightly larger than for argon and significantly lower than for xenon. Other ionic product channels that could be indicative of the occurrence of the $deNO_x$ process (reaction 1), such as CuO^+, CuN^+, CuO_2^+, and CuN_2^+, for example, were carefully looked for but not detected in the examined range of center-of-mass energies,

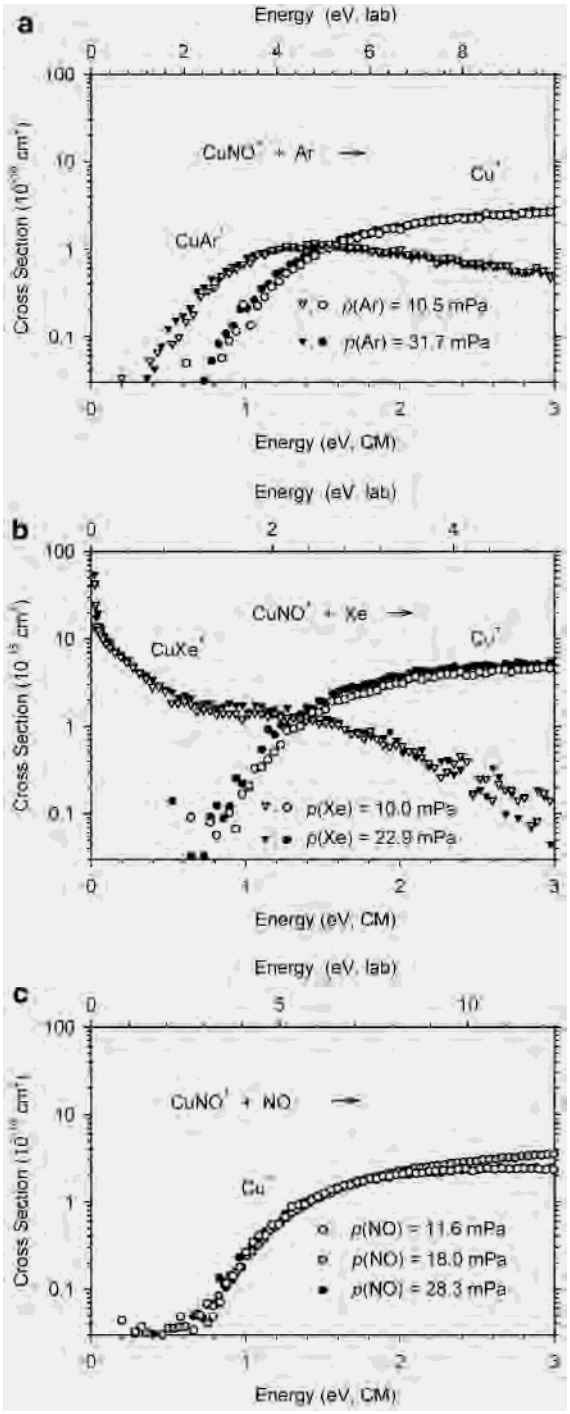

Figure 1. Product cross sections for the formation of Cu^+ (circles) and $CuRg^+$ (triangles) in the reactions of $CuNO^+$ with (a) argon, (b) xenon, and (c) nitric oxide as a function of kinetic energy in the center-of-mass (lower axis) and the laboratory (upper axis) frames at different pressures of the neutral reactants.

(31) N. Aristov, and P. B. Armentrout: *J. Phys. Chem.* **1986**, *90*, 5135.
(32) Hales, D. A.; Armentrout, P. B. *J. Cluster Sci.* **1990**, *1*, 127.
(33) Böttcher, C. J. F.; Bordewijk, P. *Theory of Electric Polarization*; Elsevier: Amsterdam, 1977; Vol. II, p 332.

Table 1. Optimized Parameters of Eq 2 Determined from the GIB Data for CID (Reaction 3) and Ligand Exchange (Reaction 4) of $CuNO^+$

	neutral	p/mPa	$\sigma_0/10^{-16}$ cm^2 eV^{n-1}	E_0/eV	n
CID	Ar	10.5	3.9	1.14	1.2
		31.7	3.6[a]	1.05[a]	1.3
	Xe	10.0	7.1	1.17	1.2
		22.9	8.0	1.11	1.2
		mean	7.5 ± 2.2		
	NO	11.6	4.3	1.11	1.1
		18.0	4.6	1.11	1.3
		28.3	4.2	1.12	1.1
		mean	4.4 ± 1.3		
			average	1.13 ± 0.05[b]	
ligand exchange	Ar	10.5	2.4	0.63 ± 0.05[c]	1.5
		31.7	2.0[a]	0.53[a]	1.7

[a] Not included in averaging because of apparent contributions of multiple collisions; see text. [b] Uncertainty contains statistical (two mean standard deviations) and systematic (uncertainty in energy scale and uncertainty of calculated frequencies; see text for details) contributions. [c] Statistical component of uncertainty was estimated to equal that of CID experiments.

$E(\mathrm{CM}) = 0-25$ eV. On the basis of the signal-to-noise ratios observed, an upper limit for their cross sections is estimated to be 0.05×10^{-16} cm^2.

In the quantitative analysis of the GIB data according to eq 2, the absence of kinetic barriers in excess of the thermochemical thresholds is postulated, as is generally assumed reasonable for simple ion−molecule reactions.[18,36] Consideration of lifetime effects in the CID channels by means of an RRKM treatment (assuming a loose transition structure in the phase-space limit)[21,22] increases the thresholds by only $\Delta E_0 \leq 0.002$ eV. Hence, virtually all energized molecules can decompose in the time window of the experiment, once sufficient internal energy is available. Moreover, the thresholds derived from the experiments using the three different neutral gases at several pressures do not show any systematic variations (Table 1), except for the highest argon pressure, $p(\mathrm{Ar}) = 31.7$ mPa, at which a threshold significantly lower than the others is obtained, indicating notable contributions of multiple collisions. If these data are discarded, the arithmetic average of the individual E_0 values is assumed to give the most accurate threshold for the dissociation of $CuNO^+$. For the range of uncertainty, a statistical component resulting from the spread of the individual E_0 values (quantified as two mean standard deviations) and systematic contributions (error of the absolute energy scale in the laboratory frame, $\Delta E(\mathrm{lab}) \approx 0.05$ eV, assumed relative error of the calculated frequencies of the reactant, $\Delta\nu_i(CuNO^+)/\nu_i(CuNO^+) = 20\%$) is considered according to laws of error propagation. Thus, $D_0(Cu^+-NO) = 1.13 \pm 0.05$ eV is obtained (Table 1). For the absolute reaction cross sections, the relative uncertainties are estimated to be 30%. Taking the arithmetic averages of the σ_0 values derived for the different pressures results in $\sigma_0(\mathrm{Ar}) = (3.9 \pm 1.2) \times 10^{-16}$ cm^2, $\sigma_0(\mathrm{Xe}) = (7.5 \pm 2.2) \times 10^{-16}$ cm^2, and $\sigma_0(\mathrm{NO}) = (4.4 \pm 1.3) \times 10^{-16}$ cm^2, respectively, where the trend nicely matches the associated polarizabilities of the neutrals (see above).

Table 2. Computed Bond Dissociation Energies (D_0 in eV) of $[Cu,N,O]^+$ Isomers and of $CuRg^+$ Complexes Observed in the Experiments

	B3LYP/B1[a]	B3LYP/B2	CCSD(T)/B3[b,c]
$CuNO^+$ (^{2}A′)	1.17 (0.16)	1.23	1.02 (0.08)
$CuNO^+$ (^{2}A")	1.00 (0.16)	1.02	
$CuON^+$ (^{2}A′)	0.73 (0.14)	0.77	0.61 (0.05)
$CuON^+$ (^{2}A″)	0.59 (0.14)	0.60	
$CuAr^+$	0.48 (0.01)	0.49	
$CuXe^+$	1.06 (0.01)	1.11	

[a] ZPVE contributions in parentheses. [b] ZPVE obtained at the B3LYP/B1 level. [c] Relativistic contributions (given in parentheses) obtained at the HF/B3 level included.

Quantitative analysis of ligand exchange was only performed in the case of the endothermic reaction 4 with Rg = argon. By reference to the CID experiments (see above), no lifetime effects were taken into account because these are supposed to be negligibly small, and an explicit RRKM treatment would demand the estimation of frequencies for the energized molecule $ArCuNO^+$. Modeling with eq 2 leads to $\sigma_0 = (2.4 \pm 0.7) \times 10^{-16}$ cm^2 and $E_0 = 0.63 \pm 0.05$ eV (Table 1), where the statistical contributions to the overall uncertainties are assumed to equal those of the CID channel. Accordingly, $D_0(Cu^+-Ar) = D_0(Cu^+-NO) - E_0 = 0.50 \pm 0.07$ eV is derived. With respect to reaction 4 with Rg = Xe, it remains to mention that the experimentally observed maximum cross section $\sigma_{max} = (14 \pm 4) \times 10^{-16}$ cm^2 at lowest energies is about 1 order of magitude below the cross section $\sigma_{LGS} = 170 \times 10^{-16}$ cm^2 calculated from collision theory.[34] Hence, ligand exchange is either hindered by a barrier, which seems rather unlikely, or the reaction is slightly endothermic. If this is the case, as also suggested by theoretical calculations of the next section, it is quite reasonable to assume that the deviation of the experimentally observed cross section $\sigma_{max} = (14 \pm 4) \times 10^{-16}$ cm^2 at thermal energy from the collision limit of $\sigma_{LGS} = 170 \times 10^{-16}$ cm^2 is entirely a result of thermochemical effects. Accordingly, the basic thermodynamic relation $\Delta_r G = -RT \ln K_{eq}$ may be applied, where the equilibrium constant is substituted by $K_{eq} = \sigma_{max}/(\sigma_{LGS} - \sigma_{max})$. Thus, we arrive at $\Delta_r G_{298}(4, \mathrm{Rg} = \mathrm{Xe}) = 0.06 \pm 0.01$ eV, which is converted to an endothermicity using molecular parameters obtained in the next section.

3.2. $CuNO^+$ Cation: Theory. All theoretical approaches used indicate that Cu^+ coordination to the nitrogen atom of NO is energetically preferred compared with the oxygen bound species (Table 2), and hence we assume that the N-coordinated isomer is sampled in the experiments. The ^{2}A′ ground state of $CuNO^+$ exhibits an end-on binding mode with a bent structure (Figure 2). Deviation from linearity can be understood as a consequence of the completely filled d-shell of the metal, which does not provide acceptor orbitals for any favorable interaction with the occupied orbitals of NO. The only available acceptor orbital, the empty 4s at copper, cannot interact with the π orbitals of NO in a linear arrangement. Instead, bending to C_s symmetry allows for an interaction between the 4s orbital on Cu and the occupied π

(34) Gioumoisis, G.; Stevenson, D. P. *J. Chem. Phys.* **1958**, *29*, 292.
(35) Schröder, D.; Loos, J.; Schwarz, H.; Thissen, R.; Dutuit, O. *Inorg. Chem.* **2001**, *40*, 3161 and references therein.
(36) Armentrout, P. B.; Simons, J. *J. Am. Chem. Soc.* **1992**, *114*, 8627.

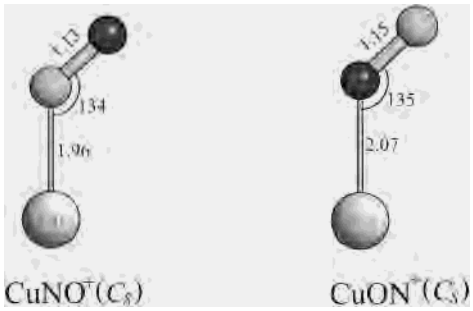

Figure 2. B3LYP/B1 structures of the lowest lying states (^{2}A′) of $CuNO^+$ and $CuON^+$. Bond lengths are given in Å, and angles, in deg.

and π^* orbitals of NO. In the ^{2}A′ ground state of $CuNO^+$ (and also $CuON^+$), the singly occupied π^* orbital can accordingly transfer electron density into the 4s orbital and thereby enhance binding. Similarly, Thomas et al. described the interaction between Cu^+ and NO in terms of a one-electron bond, where the singly occupied bonding orbital exhibits π-symmetry (the nodal plane corresponding with the plane of the molecule) with contributions from Cu 3d and 4s as well as from the NO π^* orbital.[2]

The difference of 0.06 eV between the bond energies of $CuNO^+$ (^{2}A′) obtained with B3LYP/B1 and B3LYP/B2 can be attributed to the implicit consideration of relativity in the effective core potential applied to copper in B2 as indicated by the perturbational relativistic contributions obtained at the HF/B3 level (given in parentheses in Table 2). Apparently, relativity slightly enhances binding of NO to the copper cation compared to the nonrelativistic, all-electron treatment using B1. We note in passing that application of a counterpoise correction procedure lowers both binding energies equally by 0.01 eV, thereby ruling out a major basis set superposition error (BSSE). The B3LYP/B1 value of $D_0(Cu^+-NO) = 1.17$ eV is in very good agreement with the GIB result of 1.13 ± 0.05 eV, and the B3LYP/B2 level gives $D_0(Cu^+-NO) = 1.23$ eV, slightly above the experimental error margin. A somewhat larger deviation occurs for the CCSD(T) result, which underestimates experiment. Although our calculated value agrees with CCSD(T) data reported in previous studies (ranging from 0.84[9] to 1.04 eV[10]), a T_1-diagnostic[37] of 0.025 obtained in the CCSD treatment of the SCF orbitals points to the need for the application of more advanced methods that account for the multireference character of the wave function.

For the copper cation complexes with rare gases, the DFT methods employing basis sets B1 and B2 predict $D_0(Cu^+-Ar) = 0.48$ and 0.49 eV, both values in excellent agreement with experiment, and $D_0(Cu^+-Xe) = 1.06$ and 1.11 eV, respectively. The counterpoise procedure yields minute BSSEs of 0.01 eV in all four calculations. We noted, however, a substantial underestimation of the computed polarizability of the argon atom (0.78×10^{-30} m^3) at the B3LYP/6-311+G(d) level, which is used in both basis sets applied in the present DFT calculations. A deviation of about 50% for this quantity could be a nonnegligible source of error for the computed binding energies if the charge-induced dipole interaction term ($V_{ID} = -\alpha q/8\pi\epsilon_0 r^4$, where α is the polarizability of the neutral, q is the elementary charge, ϵ_0 is the permittivity of vacuum, and r is the distance between the ion and neutral) dominates the binding, as can be expected for this type of complex. Therefore, we repeated the calculations for $CuAr^+$ employing the much more flexible aug-cc-pVTZ basis of Woon and Dunning[38] for Ar, which correctly yields $\alpha = 1.64 \times 10^{-30}$ m^3. In combination with the Stuttgart/Dresden ECP/basis for Cu, we obtain a slightly larger binding energy of $D_0(Cu^+-Ar) = 0.54$ eV, which falls inside the experimental error bars, just as the B1 and B2 results do. The counterpoise procedure again indicates an insignificant BSSE of 0.01 eV. For Xe, the applied ECP/basis combination B2 yields a correct value of $\alpha = 4.00 \times 10^{-30}$ m^3.

At both DFT levels, the predicted binding energies of $CuXe^+$ are smaller than those of $CuNO^+$ by about 0.11 eV, thus implying a slightly endothermic ligand exchange in the reaction of $CuNO^+$ with xenon. To evaluate the role of thermal contributions in the ligand exchange with atomic xenon, the enthalpies of reaction 4 with Rg = Xe were computed at the B3LYP/B2 level of theory. At 0 K, $\Delta_r H_0(4, Rg = Xe) = \Delta_r G_0(4, Rg = Xe) = 0.12$ eV is obtained, whereas $\Delta_r G_{298}(4, Rg = Xe) = 0.07$ eV, a value in excellent agreement with the experimental value obtained above, 0.06 ± 0.01 eV. Thus, replacement of NO by Xe is about 0.05 eV less endoergic at 298 K compared to 0 K, which means that our experimental value for $\Delta_r H_0(4, Rg = Xe) = 0.11 \pm 0.01$ eV. This change in thermochemistry can be associated with the particular entropic factors operative when an atom is involved in ligand exchange (see above). Thus, we obtain $D_0(Cu^+-Xe)$ by combining the experimental value $D_0(Cu^+-NO) = 1.13 \pm 0.05$ eV with $\Delta_r H_0(4, Rg = Xe)$, thereby arriving at $D_0(Cu^+-Xe) = 1.02 \pm 0.06$ eV.

3.3. $Cu(NO)_2^+$ Cation: Experiment. In analogy to reaction 3, the reactions of $Cu(NO)_2^+$ with argon and xenon under GIB conditions (Figure 3) result in the loss of one NO ligand, reaction 5. Ligand exchange is only observed in the case of xenon (reaction 6), where again no indications for the operation of kinetic barriers are obvious.

$$Cu(NO)_2^+ + Rg \rightarrow CuNO^+ + NO + Rg \qquad (5)$$

$$Cu(NO)_2^+ + Xe \rightarrow XeCuNO^+ + NO \qquad (6)$$

Whereas the experimental cross section for CID with xenon, $(23 \pm 7) \times 10^{-16}$ cm^2, is again slightly larger than that for argon, $(17 \pm 5) \times 10^{-16}$ cm^2, the difference caused by the different polarizabilities of the collision gases is less pronounced for $Cu(NO)_2^+$ in comparison to $CuNO^+$ (Table 1).

For the reaction of $Cu(NO)_2^+$ with NO, only the CID product $CuNO^+$ but no other products indicative of reactions relevant for the deNO_x process (see above) could be observed, indicating that the latter have cross sections less than about 0.1×10^{-16} cm^2 over the range of energies investigated, $E(CM) = 0-25$ eV. It is important to note that

(37) Lee, T. J.; Taylor, P. R. *Int. J. Quantum Chem. Symp.* **1989**, *23*, 199.
(38) Woon, D. E.; Dunning, T. H., Jr. *J. Chem. Phys.* **1993**, *98*, 1358.

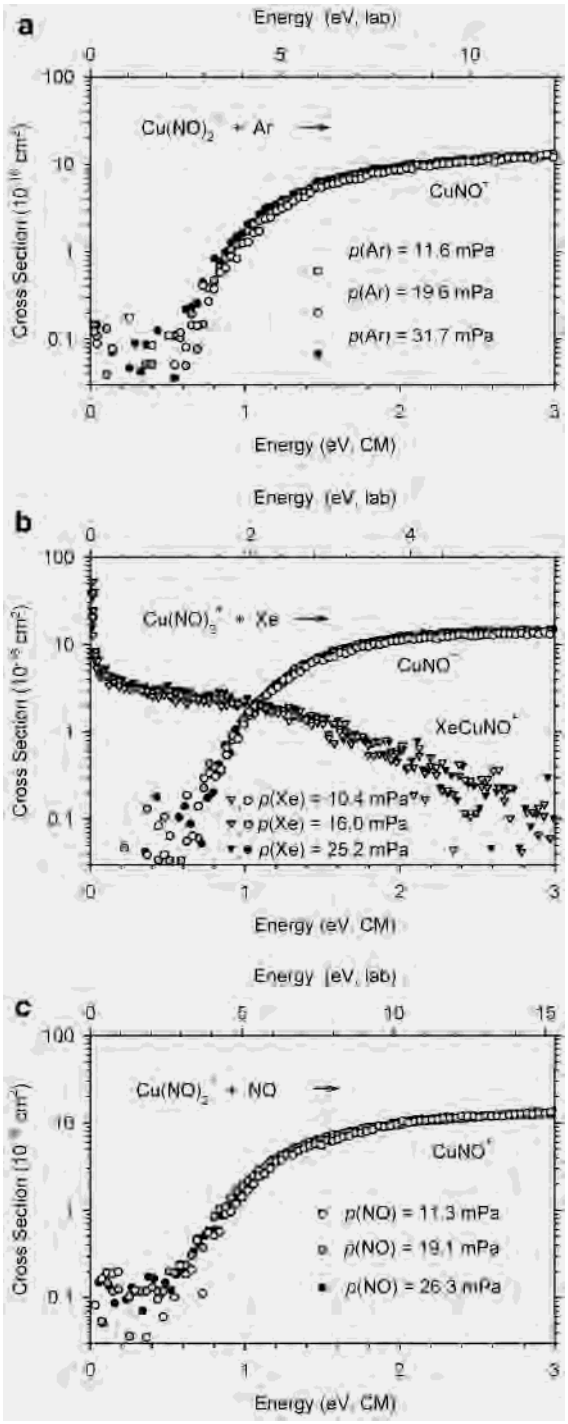

Figure 3. Product cross sections for the formation of $CuNO^+$ (circles) and $XeCuNO^+$ (triangles) in the reactions of $Cu(NO)_2^+$ with (a) argon, (b) xenon, and (c) nitric oxide as a function of kinetic energy in the center-of-mass (lower axis) and the laboratory (upper axis) frames at different pressures of the neutral reactants.

even intermediate coordination of three molecules of nitric oxide to a copper(I) center in the reaction of $Cu(NO)_2^+$ with NO obviously cannot promote any detectable bond-forming reactions in terms of the $deNO_x$ process.

In the quantitative analysis of the $Cu(NO)_2^+$ data, lifetime effects were again found to be negligible, $\Delta E_0 = 0.003$ eV. Similar to the situation with $CuNO^+$, the thresholds obtained for CID of $Cu(NO)_2^+$ with all three neutrals agree nicely with each other (Table 3) and are thus assumed to reflect

Table 3. Optimized Parameters of Eq 2 Determined from the Analysis of the GIB Data for CID (Reaction 5) of $Cu(NO)_2^+$

neutral	p/mPa	$\sigma_0/10^{-16}$ cm^2 eV^{n-1}	E_0/eV	n
Ar	11.6	16.9	1.12	1.2
	19.6	17.7	1.12	1.1
	31.7	17.2[a]	1.06[a]	1.2
	mean	17 ± 5		
Xe	10.4	22.0	1.13	1.2
	16.0	23.7	1.16	1.1
	25.2	24.7	1.15	1.2
	mean	23 ± 7		
NO	11.3	18.1	1.11	1.2
	19.1	17.6	1.07	1.1
	26.3	18.6	1.11	1.1
	mean	18 ± 5		
		average	1.12 ± 0.06[b]	

[a] Not included in averaging because of apparent contributions of multiple collisions. [b] Uncertainty contains statistical (two mean standard deviations) and systematic (uncertainty in energy scale and uncertainty of calculated frequencies; see text for details) contributions.

single-collision conditions, except the data collected at highest argon pressure, $p(\mathrm{Ar}) = 31.7$ mPa. Upon averaging of the thresholds, $D_0(\mathrm{ONCu^+{-}NO}) = 1.12 \pm 0.06$ eV is obtained. By analogy to the above analysis of reaction 4 with Rg = Xe, the cross section of the ligand-exchange reaction 6, $\sigma_{max} = (6 \pm 2) \times 10^{-16}$ cm^2, is significantly lower than the collision limit of $\sigma_{LGS} = 170 \times 10^{-16}$ cm^2, thus suggesting that reaction 6 is slightly endothermic. Using the formalism outlined above leads to an estimate of $\Delta_r G_{298}(6) = 0.09 \pm 0.02$ eV; again entropic factors may enhance the occurrence of reaction 6 at thermal energy.

3.4. $Cu(NO)_2^+$ Cation: Theory. The computational examination of $[Cu,N_2,O_2]^+$ confirms the ambident nature of the NO ligand. As for $CuNO^+$, coordination at nitrogen is found to be favored over O-coordination in $Cu(NO)_2^+$. All three isomers resulting from the different modes of N- and O-coordination are considered in their lowest singlet and triplet states (Figure 4). Overall, pleasing agreement with a maximum deviation of 0.14 eV emerges for the first NO dissociation energies of all six species investigated by B3LYP/B1, B3LYP/B2, and CCSD(T)/B3, respectively (Table 4). Moreover, the orders of stabilities for the different isomers and states almost perfectly match at these three levels; the only exception concerns ^{1}B and ^{3}C which are close in energy. Throughout the theoretical levels applied, ^{3}A clearly is the most stable complex, which is therefore assigned to be the structure sampled experimentally. The energy demands computed for loss of one NO molecule from ^{3}A, $D_0(\mathrm{ONCu^+{-}NO}) = 1.15$ eV (B3LYP/B1), 1.15 eV (B3LYP/B2), and 1.17 eV (CCSD(T)), respectively, match with 1.12 ± 0.06 eV derived from the GIB experiments. DFT predicts C_2 symmetry for ^{3}A with Cu−N distances even shorter than in the monoligated species; i.e., $r_{CuN} = 1.93$ versus 1.96 Å. The most notable aspect of the energetically higher lying isomers studied is the fact that all singlet species form cyclic structures in which bonds between the two NO entities are preformed. This finding points to an enhanced stabilization by interaction of the unpaired electrons of the NO ligands. Although N−N- and O−O-bond formations are of prime interest in the context of $deNO_x$ processes, the

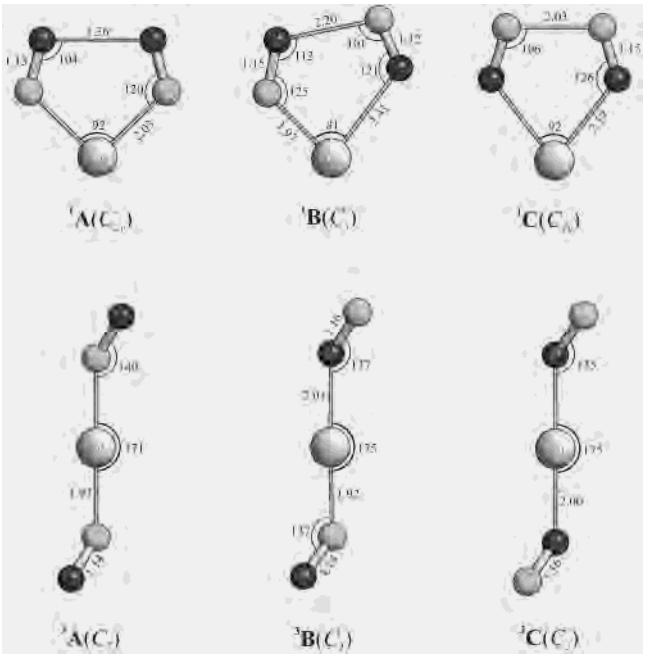

Figure 4. B3LYP/B1 structures of the lowest lying singlet and triplet states of the N- and O-coordinated $Cu(NO)_2^+$ isomers A−C. Bond lengths are given in Å, and angles, in deg.

Table 4. Computed Bond Dissociation Energies (D_0 in EV) of N- and O-Coordinated $Cu(NO)_2^+$ Isomers A−C[a]

species	B3LYP/B1[b]	B3LYP/B2	CCSD(T)/B3[c,d]
^{1}A, $ONCuNO^+$	0.55 (0.37)	0.61	0.61 (0.20)
^{1}B, $ONCuON^+$	0.16 (0.37)	0.22	0.30 (0.14)
^{1}C, $NOCuON^+$	0.00 (0.36)	0.00	0.11 (0.05)
^{3}A, $ONCuNO^+$	1.15 (0.33)	1.15	1.17 (0.16)
^{3}B, $ONCuON^+$	0.73 (0.32)	0.73	0.74 (0.14)
^{3}C, $NOCuON^+$	0.28 (0.29)	0.27	0.28 (0.09)

[a] All values given relative to $CuNO^+$ (^{2}A′) + NO ($^2\Pi$). [b] ZPVE contributions in parentheses. [c] Geometries and ZPVE obtained at the B3LYP/B1 level. [d] Relativistic contributions (given in parentheses) obtained at the HF/B3 level included.

singlet structures are, however, significantly higher in energy than the most stable isomer ^{3}A.

4. Discussion

To understand the thermochemistry of the Cu^+ complexes with NO, we first position the NO ligand into a scale of other, similarly small, but closed-shell ligands interacting with gaseous Cu^+ (Table 5). To this end, we compare the copper-ion affinities of various ligands, i.e. $D_0(Cu^+\text{-L})$, with the proton affinities (PAs) of the neutral ligands.[39] As seen in Figure 5, the NO ligand matches the previously established correlation between $D_0(Cu^+-L)$ and PA(L).[40,41] A very similar correlation evolves for the bisligated complexes (not shown). Accordingly, the open-shell character of nitric oxide has no particular effect on its binding to the monovalent transition-metal cation Cu^+. The relative weakness of the bonding between Cu^+ and NO may be appreciated by comparing it with the bond in $CuXe^+$. As shown above, the

Table 5. Sequential (D_0) and Differential (ΔD_0) Bond Dissociation Energies of CuL_2^+ Complexes and Proton Affinities PA(L) with All Values in eV

L	$D_0(Cu^+-L)$	$D_0(LCu^+-L)$	$\Delta D_0(L)$[a]	ref	PA(L)[b]
He	0.082[c]	0.096[c]	0.01[c]	46	1.82
Ar	0.50 ± 0.07			this work	3.83
	0.392[c]	0.458[c]	0.06[c]	46	
Kr	0.581[c]	0.631[c]	0.05[c]	46	4.40
Xe	1.02 ± 0.07			this work	5.18
NO	1.13 ± 0.05	1.12 ± 0.06	−0.01	this work	5.51
CO	1.54 ± 0.07	1.78 ± 0.03	0.24	48	6.16
C_2H_4	1.82 ± 0.15	1.80 ± 0.13	−0.02	49	7.05
H_2O	1.66 ± 0.01	1.76 ± 0.02	0.10	50	7.16
DME	1.92 ± 0.12	2.00 ± 0.08	0.08	51	8.21
NH_3	2.46 ± 0.15	2.55 ± 0.10	0.09	52	8.85

[a] $\Delta D_0(L) = D_0(LCu^+-L) - D_0(Cu^+-L)$. [b] Taken from ref 39. [c] D_e and ΔD_e, respectively, instead of D_0 and ΔD_0, respectively.

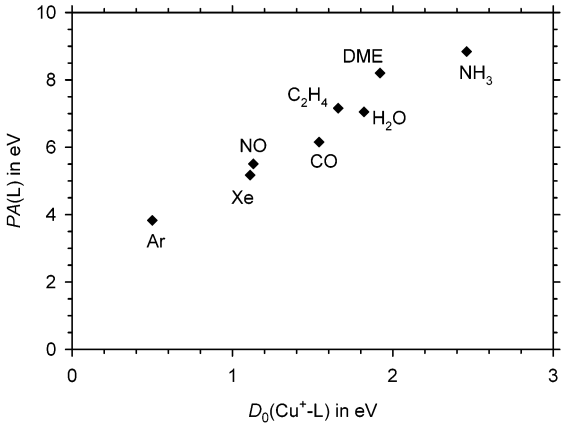

Figure 5. Correlation of experimental $D_0(Cu^+-L)$ bond energies with proton affinities PA(L), both in eV.

rare gas xenon exhibits an affinity for Cu^+ similar to that of the classical inorganic ligand NO, whereas argon binds about half as strongly to Cu^+, consistent with the larger polarizability of xenon. As one might anticipate, much stronger bonds are formed with typical Lewis bases such as water, dimethyl ether (DME), and ammonia (Table 5).

For the second NO ligand, we established a binding energy essentially equal to the first, i.e., $D_0(ONCu^+-NO) \approx D_0(Cu^+-NO)$, which might be surprising upon first sight. Generally, because of valence or charge saturation and interligand repulsion, an increase of coordination number is associated with a decrease in sequential binding energies. This particularly holds true for ionic complexes in which electrostatic interaction provides a significant contribution to the binding energy, e.g., as in the hydrated alkali-metal cations.[42] However, for transition metal complexes in general[43−45] and CuL_n^+ complexes in particular,[46−52] it is a

(39) Hunter, E. P. L.; Lias, S. G. *J. Phys. Chem. Ref. Data* **1998**, *27*, 413.
(40) Jones, R. W.; Staley, R. H. *J. Am. Chem. Soc.* **1982**, *104*, 2296.
(41) Luna, A.; Amekraz, B.; Morizur, J. P.; Tortajada, J.; Mó, O.; Yáñez, M. *J. Phys. Chem. A* **2000**, *104*, 3132 and references therein.
(42) Dzidic, I.; Kebarle, P. *J. Phys. Chem.* **1970**, *74*, 1466.
(43) Magnera, T. F.; David, D. E.; Michl, J. *J. Am. Chem. Soc.* **1989**, *111*, 4100.
(44) Marinelli, P. J.; Squires, R. R. *J. Am. Chem. Soc.* **1989**, *111*, 4101.
(45) Bauschlicher, C. W., Jr.; Langhoff, S. R. In *Gas-Phase Metal Reactions*; Fontijn, A., Ed.; North-Holland: Amsterdam, 1992; p 277.
(46) Bauschlicher, C. W., Jr.; Partridge, H.; Langhoff, S. R. *Chem. Phys. Lett.* **1990**, *165*, 272.
(47) Bauschlicher, C. W., Jr.; Langhoff, S. R.; Partridge, H. *J. Chem. Phys.* **1991**, *94*, 2068.
(48) Meyer, F.; Chen, Y.-M.; Armentrout, P. B. *J. Am. Chem. Soc.* **1995**, *117*, 4071.

well-known phenomenon that the second ligand is equally or even more strongly bound than the first; see the ΔD_0(L) column in Table 5. Bauschlicher et al. investigated this trend computationally and established a binding mechanism that involves s/d hybridization on the transition-metal center.[46,47] Thereby, two hybrid orbitals are formed from the doubly occupied $3d_{z^2}$ and the empty 4s orbital on ground-state $Cu^+(^1S)$. Through occupation of the $4s-3d_{z^2}$ hybrid, formerly spherically symmetric d-electron density is polarized away from the metal−ligand bond axis, which leads to a deshielding of the nuclear charge in this direction and enhanced electrostatic interactions. The unoccupied $4s + 3d_{z^2}$ hybrid, in turn, has an improved spatial extent along the bond axis and can therefore serve as a highly efficient acceptor orbital for electron density from the ligand. Such hybridization actually represents an admixture of the second excited ^1D state ($3d^94s^1$) to the ground state ^1S ($3d^{10}4s^0$) wave function of Cu^+. Accordingly, formation of the hybrid orbitals is connected with an s ← d promotion of electrons and the energetic costs are balanced against the gain in energy resulting from improved electrostatic interactions and orbital overlap. In transition-metal complexes, the costs are paid primarily by the first ligand, whereas the second, in a linear coordination mode, can profit for free. As only two ligands can adopt a linear coordination mode, a third ligand does not benefit from ds−σ hybridization and thus forms a much weaker bond; for instance, $D_0((OC)_{n-1}Cu^+-CO) = 1.54 \pm 0.07$, 1.78 ± 0.03, and 0.78 ± 0.04 eV for $n = 1-3$.[48] This bonding concept has generally been very successful in explaining trends for sequential binding energies of gas-phase transition-metal complexes.[53,54]

As shown above, the experimental data and the theoretical predictions agree reasonably well for all Cu^+ compounds examined here. However, a note of caution must be added to the CCSD(T)/B3 results because all six calculations are characterized by T_1-diagnostics that lie between 0.025 and 0.031, exceeding the recommended limit of 0.020[37] indicative of well-behaved single-reference cases. It has been noted that DFT can cope to a certain extent with electronic situations actually requiring a multireference Ansatz for the wave function in post-HF calculations.[55] On the other hand, it has repeatedly been shown that the B3LYP functional tends to artificially favor high spin over low-spin states, which could qualify the accuracy of computed singlet/triplet gaps.[55] Notwithstanding such concern, the good agreement between CCSD(T) and B3LYP data generally substantiates the validity of computed energetics and supports the assignments for the present cases.

Table 6. Relative Thermochemistry (E_{rel} in EV) of Several Products Which Might Possibly Form from $Cu(NO)_2^+$

species	E_{rel}[a]
$Cu(NO)_2^+$	0.00
$Cu(NO)^+ + NO$	1.12 ± 0.06
$Cu(N_2)^+ + O_2$	-0.53 ± 0.32[b]
$Cu(O_2)^+ + N_2$	-0.39[c]
$CuO^+ + N_2O$	2.48 ± 0.12[b]
$CuN^+ + NO_2$	4.11 ± 0.11[b,d]
	4.81[e]
$Cu^+ + O_2 + N_2$	0.39 ± 0.08
$Cu^+ + 2NO$	2.25 ± 0.08

[a] Δ_fH values of the neutrals taken from: Lide, D. R., Jr. *J. Phys. Chem. Ref. Data* **1988**, *17*, 1. [b] Taken from: Rodgers, M. T.; Walker, B.; Armentrout, P. B. *Int. J. Mass Spectrom.* **1999**, *182/183*, 99. [c] Taken from ref 9. [d] Formation of $CuN + NO_2^+$ is a viable alternative; see text. [e] Theoretical data suggest $E_{rel} = 4.81$ eV for this channel; see: Luna, A.; Alcamí, M.; Mí, O.; Yáñez, M. *Chem. Phys. Lett.* **2000**, *320*, 129.

Finally, none of the experiments described here yields any evidence for the occurrence of reactions that could be associated with the $deNO_x$ process described in the Introduction. Nevertheless, combination of the present results with literature data allows the estimation of the relevant thermochemistry of putative $deNO_x$ products involving gas-phase catalysis by bare Cu^+ ions (Table 6). Even without consideration of reaction barriers, the thermochemistry predicts that the only exothermic reactions of $Cu(NO)_2^+$ are the formations of $Cu(O_2)^+ + N_2$ and $Cu(N_2)^+ + O_2$, respectively. All other putative products of bond metathesis, such as $CuO^+ + N_2O$ or $CuN^+ + NO_2$, are much higher in energy. Because of the relatively low ionization energy of NO_2, $CuN + NO_2^+$ is also an energetically viable dissociation asymptote, but no quantitative information on gaseous CuN is available.[56] Above $D_0(ONCu^+-NO) = 1.12 \pm 0.06$ eV, energized $Cu(NO)_2^+$ will almost certainly dissociate by simple loss of NO. Hence, rearrangement channels of relevance to the $deNO_x$ process are only likely to compete if they bear activation energies lower than $D_0(ONCu^+-NO)$. In this respect, the dissociation asymptotes for $CuO^+ + N_2O$ and $CuN^+ + NO_2$ imply that also the putative intermediates $CuO(N_2O)^+$ and $CuN(NO_2)^+$, respectively, are unlikely to be located below this energy limit because N_2O is a weakly coordinating ligand and the $CuN^+ + NO_2$ asymptote is high in energy. Accordingly, thermochemical considerations clearly suggest that stepwise sequences of N−N- and O−O-bond formations are inaccessible for energized $Cu(NO)_2^+$ in its ^3A state. Only a direct, concerted process in which N−O bond cleavages and formation N_2 and O_2 occur more or less simultaneously could provide a low-lying access to the $deNO_x$ route. However, such a direct process is symmetry forbidden and connected with substantial barriers.[57] Further, consideration of the calculated structures implies that only the singlet isomers are likely to react in this manner, which would, in turn, require spin-crossover in the course of the

(49) Sievers, M. R.; Jarvis, L. M.; Armentrout, P. B. *J. Am. Chem. Soc.* **1998**, *120*, 1891.
(50) Dalleska, N. F.; Honma, K.; Sunderlin, L. S.; Armentrout, P. B. *J. Am. Chem. Soc.* **1994**, *116*, 3519.
(51) Koizumi, H.; Zhang, X.-G.; Armentrout, P. B. *J. Phys. Chem. A* **2001**, *105*, 2444.
(52) Walter, D.; Sievers, M. R.; Armentrout, P. B. *J. Am. Chem. Soc.* **1998**, *120*, 3176.
(53) Bauschlicher, C. W.; Langhoff, S. R.; Partridge, H. In *Modern Electronic Structure Theory*; Yarkony, D. R., Ed.; World Scientific: Singapore, 1995; Part II.
(54) Rodgers, M. T.; Armentrout, P. B. *Mass Spectrom. Rev.* **2000**, *19*, 215.
(55) Koch, W.; Holthausen, M. C. *A Chemist's Guide to Density Functional Theory*; Wiley-VCH: Weinheim, Germany, 2001.
(56) Bera, J. K.; Samuelson, A. G.; Chandrasekhar, J. *Organometallics* **1998**, *17*, 4136.
(57) Tajima, N.; Hashimoto, M.; Toyama, F.; El-Nahas, A. M.; Hirao, K. *Phys. Chem. Chem. Phys.* **1999**, *1*, 3823.

reaction.[58] On the basis of the experimental results, we therefore conclude that these restrictions cannot be surmounted in $Cu(NO)_n^+$ with n up to 3.

5. Conclusions

By means of guided ion beam mass spectrometry, the bond dissociation energies of $CuNO^+$, $Cu(NO)_2^+$, and $CuAr^+$ are determined as $D_0(Cu^+-NO) = 1.13 \pm 0.05$, $D_0(ONCu^+-NO) = 1.12 \pm 0.06$, and $D_0(Cu^+-Ar) = 0.50 \pm 0.07$ eV. These results agree well with binding energies obtained by density functional theory and coupled-cluster theory. By measuring the equilibrium constant for ligand exchange of NO and Xe and combining this with appropriate molecular parameters, we also obtain $D_0(Cu^+-Xe) = 1.02 \pm 0.06$ eV.

On the basis of the present results, gaseous Cu^+ ions cannot induce occurrence of the $deNO_x$ process of nitric oxide (reaction 1) because of kinetic barriers and/or spin-inversion restrictions. Although it would be very attractive to experimentally enter the potential-energy surface from an alternative side, e.g., $CuO^+ + N_2O$ or $CuN^+ + NO_2$, no efficient means to generate the requisite ionic precursors are available for the time being. Hence, development of alternative ionization schemes to generate these species would be of great interest. As far as theory is concerned, the investigation of possible reaction paths connecting $Cu(NO)_2^+$ and $Cu(N_2)(O_2)^+$ quite obviously requires much higher levels of sophistication than single-reference-based CCSD(T), as will be presented in a future study.[59]

In a more general sense, failure to observe $deNO_x$ reactivity in the Cu^+/NO system under the idealized conditions of gas-phase experiments indicates that either (i) more than a single copper atom is required to drive the $deNO_x$ process,[60] (ii) participation of the backbone (e.g. zeolites) or solvents (e.g. proton catalysis) in the reaction is essential, or (iii) the active species is not Cu(I) but either Cu(0) or Cu(II),[57] both open-shell species that may induce covalent binding with the NO radical.

Acknowledgment. This work has financially been supported by the Deutsche Forschungsgemeinschaft, the Fonds der Chemischen Industrie, and the National Science Foundation (P.B.A., Grant CHE-013557). The Fonds der Chemischen Industrie is particularly acknowledged for a Kekulé-Scholarship (K.K.) and a Liebig-Stipendium (M.C.H.).

Note Added after Print Publication: Due to a production error, several reference numbers in the text were incorrect in the version of this paper published on the Web on 10/05/2002 (ASAP) and in the November 4, 2002, issue (Vol. 41, No. 22, 5882−5890). The following changes were made. Page 5883: 14 to 20; 15 and 16 near the bottom of the left-hand column to 21 and 22; 21 to 27. Page 5884: 28 to 34; 29 to 35. Page 5886: 31 to 37. Page 5888: 33 to 39. The correct reference numbers are present in the version posted on 11/27/2002, and an Addition and Correction appears in the December 30, 2002, issue (Vol. 41, No. 26).

IC020315A

(58) Schröder, D.; Shaik, S.; Schwarz, H. *Acc. Chem. Res*. **2000**, *33*, 139 and references therein.
(59) Holthausen, M. C. Manuscript in preparation.
(60) Spuhler, P.; Holthausen, M. C.; Nachtigallova, D.; Nachtigall, P.; Sauer, J. *Chem.—Eur. J*., in press.